NASA TECHNICAL MEMORANDUM

NASA TM X-2541

NASA TM X-2541
c.1

ANALYSIS OF THE EFFECT OF ENGINE CHARACTERISTICS ON THE EXTERNAL AERODYNAMICS OF STOL WING PROPULSION SYSTEMS

by James A. Albers

Lewis Research Center
Cleveland, Ohio 44135

NATIONAL AERONAUTICS AND SPACE ADMINISTRATION • WASHINGTON, D. C. • APRIL 1972

1. Report No. NASA TM X-2541	2. Government Accession No.	3. Recipient's Catalog No.
4. Title and Subtitle ANALYSIS OF THE EFFECT OF ENGINE CHARACTERISTICS ON THE EXTERNAL AERODYNAMICS OF STOL WING PROPULSION SYSTEMS		5. Report Date April 1972 6. Performing Organization Code
7. Author(s) James A. Albers		8. Performing Organization Report No. E-6757
9. Performing Organization Name and Address Lewis Research Center National Aeronautics and Space Administration Cleveland, Ohio 44135		10. Work Unit No. 741-72 11. Contract or Grant No.
12. Sponsoring Agency Name and Address National Aeronautics and Space Administration Washington, D.C. 20546		13. Type of Report and Period Covered Technical Memorandum 14. Sponsoring Agency Code
15. Supplementary Notes		

16. Abstract

The effects of engine pressure ratio, engine size, and engine location on the pressure distribution, lift coefficient, and flow field of a STOL wing propulsion system are presented. The flow variables of the engines are included in the two-dimensional potential flow analysis by considering the effects of mass flow coefficient at the engine inlet and thrust coefficient at the engine exit. A functional relation between these coefficients and engine pressure ratio is given. The results of this study indicate that the effect of engine pressure ratio on the external aerodynamics is a function of engine location. For engines located on the bottom of the wing, the highest pressure ratio engine resulted in the highest lift coefficient. For engines located on the top of the wing, the lowest pressure ratio engine resulted in the highest lift coefficient.

17. Key Words (Suggested by Author(s))		18. Distribution Statement
STOL	Aerodynamics, external	Unclassified - unlimited
Propulsion system	Potential flow	
Engine pressure ratio	Pressure distribution	
Jet flap		

19. Security Classif. (of this report)	20. Security Classif. (of this page)	21. No. of Pages	22. Price*
Unclassified	Unclassified	19	$3.00

* For sale by the National Technical Information Service, Springfield, Virginia 22151

ANALYSIS OF THE EFFECT OF ENGINE CHARACTERISTICS ON THE EXTERNAL AERODYNAMICS OF STOL WING PROPULSION SYSTEMS

by James A. Albers

Lewis Research Center

SUMMARY

The effects of engine pressure ratio, engine size, and engine location on the pressure distribution, lift coefficient, and flow field of a STOL wing propulsion system are presented. The flow variables of the engines are included in the two-dimensional potential flow analysis by considering the effects of mass flow coefficient at the engine inlet and thrust coefficient at the engine exit. A functional relation between these coefficients and engine pressure ratio is given. The results of this study indicate that the effect of engine pressure ratio on the external aerodynamics is a function of engine location. For engines located on the bottom of the wing, the highest pressure ratio engine resulted in the highest lift coefficient. For engines located on the top of the wing, the lowest pressure ratio engine resulted in the highest lift coefficient.

INTRODUCTION

The external aerodynamics of combined wing and propulsion systems under high lift conditions are needed to do detailed design studies of STOL configurations. Because of the expense and complexity of models of powered high lift systems, only a limited range of design variables and geometries can be tested in the wind tunnel. The external aerodynamics can also be determined from a potential flow analysis that includes the effects of engine characteristics. This report considers an analysis of two-dimensional wing propulsion systems which consist of an airfoil and flap; the engines, which have a distributed suction at their inlet and a jet at their exit; and a jet sheet leaving the flap trailing edge. With such a potential flow analysis, the designer can consider a wide variety of configuration variables at modest cost and develop an understanding of many significant factors contributing to the design of wing propulsion systems. By combining this potential flow analysis with an airplane performance and boundary layer analysis,

the designer is better equipped to select the (1) wing propulsion system, (2) engine location and orientation, (3) engine pressure ratio and size, and (4) airfoil geometry.

A potential flow theory often used when considering STOL wing propulsion systems is the jet flap theory as discussed in references 1 and 2. This thin airfoil theory assumes small flow deflections and considers the effect of the engine exhaust jet but does not take into account the effect of the engine inlet. A more recent potential flow solution for a combination engine-wing system is presented in reference 3. This solution includes the following four effects: (1) inlet airflow of the propulsion system, (2) exhaust jet of the propulsion system, (3) wing thickness and camber, and (4) high wing angles of attack and large flap and flow deflection angles. By use of this solution, the effect of the engines on the wing pressure distribution and lift coefficient can be obtained.

The purpose of this report is to investigate the effects of the flow variables of the engine on the external aerodynamics of the combined wing and propulsion system. The flow variables of the engine are treated by considering the effects of thrust coefficient at the propulsion system exhaust and mass flow coefficient at the propulsion system inlet. A functional relation between these coefficients and engine pressure ratio is given.

This report presents the effects of engine pressure ratio, engine size, and engine location on the pressure distribution, lift coefficient, and flow field. Engine pressure ratios range from 1.08 to 1.34 with three engine locations: under the wing, near the wing leading edge, and on top of the wing flap. The present study was made for a free-stream Mach number of 0.12, zero wing angle of attack (NACA 4415 airfoil with flap), and 30° jet incidence angle at the flap trailing edge. Comparisons of predicted lift coefficients with jet flap theory and with experimental data are also included.

SYMBOLS

C_L three-dimensional lift coefficient

C_l two-dimensional lift coefficient

C_p pressure coefficient

C_Q mass flow coefficient

C_T thrust coefficient

c chord length (fig. 1)

M Mach number

$\dot{m}$ fan or engine mass flow rate per unit span

P total pressure

p static pressure

T total temperature

t static temperature

$\bar{t}$ wing thickness

V velocity

x distance along wing chord

y distance normal to wing chord

α angle of attack

γ ratio of specific heats

θ flap angle (fig. 1)

η adiabatic efficiency

ρ free-stream density

Subscripts:

e engine exit

o engine inlet

∞ free stream

METHOD OF ANALYSIS

For any STOL wing propulsion system, the engine is an integral part of the lifting system. This complicates the mathematical analysis needed for a reasonable approximation to the physical system. Although the effect of the engine is three-dimensional, the presented two-dimensional analysis contains the basic characteristics of wing-engine systems. For multiple engine-wing propulsion systems and two-dimensional ejectors located at the wing trailing edge, as the augmentor wing, it is reasonable to approximate the wing section flow characteristics with a two-dimensional flow.

A representation of a typical two-dimensional lifting system is shown in figure 1. The wing propulsion system combination is idealized by considering it to be one solid body with suction at the propulsion system inlet. Since the exhaust jet of the propulsion system is at a higher total pressure than the surrounding flow and potential flow presumes a uniform total pressure, the jet is considered to be a part of the solid body. The potential flow is calculated for a body surface, which consists of an airfoil with flap; the engines or fans, which have a distributed suction at their inlet and a jet at their exit; and a jet sheet leaving the flap trailing edge. The analysis was accomplished by extension of the two-dimensional Douglas program (refs. 4 and 5) to include the effect of suction

at the propulsion system inlet, and by the development of a technique for determining the approximate location of the exhaust jet of the propulsion system (ref. 3). The effect of suction was obtained by combining the Douglas basic suction solution with a uniform flow solution for a lifting body. The location of the jet exhaust was determined by balancing the vertical component of thrust at the flap with the integrated vertical pressure forces on the free jet. A description of the computer program used to obtain the solution is given in reference 6.

The potential flow problem for a given wing propulsion system is one of calculating the velocities on and external to the body for any combination of the following variables: (1) free-stream velocity V_∞; (2) fan or engine mass flow rate per unit span $\dot{m}$; (3) propulsion system exit momentum (thrust) per unit span; (4) flap angle θ; and (5) wing angle of attack α. The first three variables can be combined into two dimensionless parameters: the engine or fan mass flow coefficient $C_Q = \dot{m}/\rho V_\infty c$, and the exit thrust coefficient $C_T = \dot{m}V_e/(1/2\rho V_\infty^2 c)$. The relation between these two parameters and the propulsion system parameter of engine pressure ratio P_e/P_o can be expressed as

$$\frac{C_Q}{C_T} = \sqrt{\frac{\gamma - 1}{8}} \frac{M_\infty}{\sqrt{1 + \frac{\gamma - 1}{2} M_\infty^2 - \left(\frac{P_e}{P_o}\right)^{-(\gamma-1)/\gamma}} \sqrt{\frac{1}{\eta}\left[\left(\frac{P_e}{P_o}\right)^{(\gamma-1)/\gamma} - 1\right] + 1}} \tag{1}$$

This equation is derived in the appendix and illustrated in figure 2 for $M_\infty = 0.12$ and $\eta = 0.85$. The figure shows that the ratio of mass flow coefficient to thrust coefficient increases with decreasing engine pressure ratio.

EFFECT OF ENGINE CHARACTERISTICS

The engine characteristics are represented by two propulsion system parameters - mass flow coefficient $C_Q = \dot{m}/\rho V_\infty c$, and exit thrust coefficient $C_T = \dot{m}V_e/(1/2\rho V_\infty^2 c)$. By use of these two parameters, both the effect of suction at the engine inlet and the effect of the exhaust jet of the engine are included in the analysis. These two propulsion system parameters are related to the engine pressure ratio (eq. (1)), an important engine characteristic. The effect of engine pressure ratio is discussed first. This is followed by a more detailed discussion of the effects of the propulsion system parameters - mass flow coefficient and thrust coefficient. For all the propulsion systems studied, the wing angle of attack is 0°, and the jet incidence angle at the wing trailing edge is 30°. The calculations were made for $M_\infty = 0.12$, which is representa-

tive of STOL takeoff and landing speeds. A representative value of fan efficiency (η = 0.85) was used in calculating engine pressure ratio.

Engine Pressure Ratio

The effect of engine pressure ratio is shown in figure 3 for engines located on top of the wing flap for a constant thrust coefficient. A constant thrust coefficient and a varying engine pressure ratio imply a varying mass flow coefficient (fig. 2). The effect of engine pressure ratio on the upper surface pressure distribution is illustrated in figure 3(a). As the engine pressure ratio is decreased from 1.34 to 1.08, the average negative value of the upper surface pressure coefficient is increased by 50 percent. Corresponding to the increase in the negative pressure coefficient, the steepness of the adverse pressure gradient at the wing leading edge also increased with the engine pressure ratio. The increase in the negative value of the pressure coefficient is due to the effect of inlet suction (increased mass flow coefficient) as engine pressure ratio is reduced. The lift coefficient increased from 6 to 6.8 as the engine pressure ratios decreased from 1.5 to 1.08 as shown in figure 3(b). Associated with the lower pressure ratio and higher values of C_Q is a thickening of the inlet flow stream tube entering the engine. This is illustrated in figure 4 for two different engine pressure ratios. As mass flow is increased (reflected by a change in engine pressure ratio), the stagnation point shifts further under the wing leading edge. There is also a larger jet penetration at the lower engine pressure ratios as shown in figure 5. This result is due to the increase in suction at the engine inlet corresponding to the lower pressure ratio.

The effect of engine pressure ratio on the upper surface pressure distribution for engines located under a wing is presented in figure 6(a). This figure indicates the opposite effect of engine pressure ratio on the pressure distribution from that shown in figure 3. As the engine pressure ratio decreased from 1.34 to 1.08, the average negative value of the upper surface pressure coefficient decreased by 20 percent. For the lower pressure ratio engine, the increase in mass flow coefficient (inlet suction of the engine) contributes to the reduction in the value of the pressure coefficient. For engines located under the wing, the higher the pressure ratio the higher the negative pressure coefficients and the more the adverse pressure gradient at the wing leading edge. The higher pressure ratio in this case gives the higher lift coefficient as shown in figure 6(b). This is opposite to the pressure ratio effect found when the engine was located on the wing flap. Thus, the effect of engine pressure ratio on the external aerodynamics is a function of engine location.

Usually in the literature (for example, see ref. 7) the effect of engine characteristics on the external aerodynamics is represented by using only the exit thrust coefficient as a parameter. It has been demonstrated in the previous discussion that for a

constant thrust coefficient the engine pressure ratio has a definite effect on the lift coefficient and pressure distribution of the wing propulsion system. Thus, when the engine inlet is in the vicinity of the wing, both engine exit thrust coefficient and engine pressure ratio should be specified when illustrating the effects of the engine on the external aerodynamics.

Engine Thrust Coefficient

The effect of thrust coefficient on pressure distribution is illustrated in figure 7 for the engines on top of the flap and for constant engine mass flow coefficient. A constant mass flow coefficient and varying engine pressure ratio imply a varying thrust coefficient (fig. 2). The average negative value of the pressure coefficient increased by 25 percent as the thrust coefficient increased from 2.6 to 4.5. An increase in thrust coefficient results in greater exhaust jet penetration and a shift in the stagnation point further under the wing leading edge. Consequently, higher lift coefficients and larger adverse pressure gradients are obtained at the larger thrust coefficients (see fig. 7(b)). Similar incremental changes in pressure would be obtained for other engine locations for the same jet incidence angle since the effect of thrust coefficient is independent of engine location.

Engine Size

For a constant engine pressure ratio the engine size is varied by the simultaneous variation of mass flow coefficient and thrust coefficient. The effect of engine size is shown for an engine pressure ratio of 1.34 in figure 8. For engines located on top of the wing (fig. 8(a)), a 50-percent increase in both thrust coefficient and mass flow coefficient results in an 80-percent increase in the negative value of the upper surface pressure coefficient. In this case, the effects of thrust coefficient and mass flow coefficient increase the negative level of the upper surface pressures. For the engine located on the bottom of the wing (fig. 8(b)), a 50-percent increase in both mass flow coefficient and thrust coefficient results in a 10-percent decrease in the negative value of the upper surface pressure coefficient. For this engine location, the effect of mass flow coefficient outweighs the effect of thrust coefficient.

Engine Location

A comparison of pressure distributions at various engine locations for an engine pressure ratio of 1.18 is presented in figure 9. For the engine located on top of the

wing flap, high negative pressure coefficients exist near the wing leading edge followed by a large adverse pressure gradient. A very mild adverse pressure gradient existed for the engine located under the wing. A relatively flat pressure profile was obtained for the engine located at the front of the wing. Lift coefficients corresponding to each pressure distribution are also given. The pressure distribution with the highest average negative value of pressure coefficient has the largest value of lift coefficient. The differences in pressure distribution and lift coefficient can be attributed to the effects of suction at the engine inlet. Flow fields for the various engine locations are illustrated in figure 10. For the engines located at the front of the wing and under the wing, one stagnation point occurs at the wing leading edge and another occurs on the under surface of the engine. For the engine located on top of the wing flap (fig. 10(c)), one stagnation point occurs slightly under the wing leading edge and the other occurs at the inlet lip of the engine. A close study of figures 10(a) and (b) reveals that the average upwash angle at the engine inlet for the engine located at the front of the wing is less than the upwash angle for the engine located under the wing. Upwash angles are important when considering the performance of the propulsion system inlet and overall engine performance.

COMPARISONS

Jet Flap Theory

A comparison of two-dimensional lift coefficients by the method of this report (with $C_Q = 0$ and no engine) and Spence's jet flap theory (ref. 2) is presented in figure 11 for various jet incidence angles. The jet flap results were corrected for wing thickness by applying the standard thickness correction $(1 + \bar{t}/c)$. Good agreement was found between the method of this report and jet flap theory for jet incidence angles of 14° and 30°, respectively. For a jet incidence angle of 60°, the lift coefficients predicted by the method of this report were, on the average, 4.5 percent higher than jet flap theory. This result is expected since the method of this report accounts for large flap deflection angles whereas jet flap theory assumes small angles.

Experiment

A comparison of predicted three-dimensional lift coefficients with experimental data is presented in figure 12. The theoretical three-dimensional lift coefficients were obtained by applying the aspect ratio correction of reference 8 to the predicted two-dimensional lift coefficients. The experimental data for both engine locations were obtained from wind tunnel tests at the NASA Lewis Research Center V/STOL propulsion

wind tunnel (see ref. 9 for wind tunnel description). A more detailed description of the test models can be found in references 3 and 10. For engines located on top of wing, the predicted lift coefficients were, on the average, 15 and 20 percent higher than the experimental data for the jet incidence angles of 14° and 30°, respectively. The predicted lift coefficients for engines located under the wing were, on the average, 11 percent higher than experimental data. Similar percent differences between potential flow predictions and experimental data on high lift wings are discussed in reference 11. It is expected that the predicted lift coefficient be greater than the experimental data, since the calculated lift coefficient is the maximum attainable, corresponding to complete boundary layer control and negligible viscous effects.

SUMMARY OF RESULTS

The effects of the engine on the external aerodynamics of STOL wing propulsion systems, as determined from two-dimensional potential flow analysis, were illustrated. For the propulsion system studied, the engine inlet was in the vicinity of the wing, the wing angle of attack was 0°, the jet incidence angle was 30°, and the free-stream Mach number was 0.12. The principal results of this study are as follows:

1. For a constant engine exit thrust coefficient, the pressure distribution and lift coefficient change with engine pressure ratio (varying mass flow coefficient). Thus, both engine exit thrust coefficient and engine pressure ratio should be specified when considering the effects of the engine on the external aerodynamics.

2. The effect of engine pressure ratio (for constant thrust coefficient and varying mass flow coefficient) on the external aerodynamics is a function of engine location. For engines located on top of the wing, the negative value of the upper surface pressure coefficients increases (resulting in greater lift coefficients) with a decrease in engine pressure ratio. For engines located on the bottom of the wing, the value of the upper surface pressure coefficient increased (resulting in greater lift coefficients) with an increase in engine pressure ratio.

3. For a constant engine pressure ratio, the same percent increase in both thrust coefficient and mass flow coefficient (an increase in engine size) resulted in an increase in the negative value of the upper surface pressure coefficient and an increase in lift coefficient for an engine located on top of the wing. For an engine located under the wing, the effect resulted in a decrease in the negative value of the upper surface pressure coefficient and lift coefficient.

4. A comparison of pressure distributions at various engine locations for an engine pressure ratio of 1.18 indicated a relatively flat pressure profile for the engine located at the front of the wing, a very mild adverse pressure gradient for the engine located

under the wing, and a large adverse pressure gradient at the wing leading edge for the engine located on top of the wing flap.

5. The average upwash angle at the engine inlet for the engine located at the front of the wing was less than for the engine located under the wing.

6. A comparison of the predicted two-dimensional lift coefficients by the method of this report and Spence's jet flap theory indicates good agreement for jet incidence angles of 14° and 30°.

7. The predicted lift coefficients ranged from 11 to 20 percent higher than the experimental lift coefficients for the wing propulsion systems tested.

Lewis Research Center,
National Aeronautics and Space Administration,
Cleveland, Ohio, February 15, 1972,
741-72.

APPENDIX - RELATION OF PROPULSION SYSTEM PARAMETERS TO ENGINE PRESSURE RATIO

In this appendix, an equation is derived which relates the ratio of mass flow coefficient C_Q to exit thrust coefficient C_T to engine pressure ratio P_e/P_o, adiabatic efficiency η, and free-stream Mach number M_∞. The propulsion system parameters are defined as

$$\left.\begin{aligned} C_Q &= \frac{\dot{m}}{\rho V_\infty c} \\ \text{and} \\ C_T &= \frac{\dot{m} V_e}{\frac{1}{2}\rho V_\infty^2 c} \end{aligned}\right\} \qquad \text{(A1)}$$

The thrust coefficient is defined at the trailing edge of the wing (fig. 1), and the exit velocity is calculated assuming that the average static pressure in the exit jet is ambient pressure ($p_e = p_\infty$). Using the definition of C_Q and C_T and the definition of the speed of sound for a perfect gas yield the ratio of the two propulsion system parameters:

$$\frac{C_Q}{C_T} = \frac{V_\infty}{2V_e} = \frac{M_\infty \sqrt{t_o}}{2M_e \sqrt{t_e}} \qquad \text{(A2)}$$

When the total to static isentropic expressions for temperature ratio (ref. 12) are used,

$$\left.\begin{aligned} \frac{T_e}{t_e} &= 1 + \frac{\gamma - 1}{2} M_e^2 \\ \text{and} \\ \frac{T_o}{t_o} &= 1 + \frac{\gamma - 1}{2} M_\infty^2 \end{aligned}\right\} \qquad \text{(A3)}$$

the expression for total exit temperature in terms total inlet stagnation temperature, adiabatic efficiency, and engine pressure ratio becomes

$$T_e = \frac{T_o}{\eta}\left[\left(\frac{P_e}{P_o}\right)^{(\gamma-1)/\gamma} - 1\right] + T_o \tag{A4}$$

The inlet total pressure and inlet total temperature are identical to the free-stream conditions ($P_o \equiv P_\infty$, $T_o \equiv T_\infty$). When equations (A2), (A3), and (A4) are combined, C_Q/C_T can be expressed as

$$\frac{C_Q}{C_T} = \frac{1}{2}\left(\frac{M_\infty^2}{1 + \frac{\gamma - 1}{2} M_\infty^2}\right)^{1/2} \frac{\sqrt{1 + \frac{\gamma - 1}{2} M_e^2}}{M_e \sqrt{\frac{1}{\eta}\left[\left(\frac{P_e}{P_o}\right)^{(\gamma-1)/\gamma} - 1\right] + 1}} \tag{A5}$$

The relation for exit Mach number in terms of pressure ratio (assuming $p_e = p_\infty$) can be expressed as

$$M_e^2 = \left[\left(\frac{P_o}{p_\infty}\frac{P_e}{P_o}\right)^{(\gamma-1)/\gamma} - 1\right]\frac{2}{\gamma - 1} \tag{A6}$$

where P_o/p_∞ is determined from the free-stream Mach number:

$$\frac{P_o}{p_\infty} = \left(1 + \frac{\gamma - 1}{2} M_\infty^2\right)^{\gamma/(\gamma-1)} \tag{A7}$$

Substituting equations (A6) and (A7) into equation (A5) yields an expression for the propulsion system parameters C_Q and C_T in terms of P_e/P_o, M_∞, and η:

$$\frac{C_Q}{C_T} = \sqrt{\frac{\gamma - 1}{8}} \frac{M_\infty}{\sqrt{1 + \frac{\gamma - 1}{2} M_\infty^2 - \left(\frac{P_e}{P_o}\right)^{-(\gamma-1)/\gamma}} \sqrt{\frac{1}{\eta}\left[\left(\frac{P_e}{P_o}\right)^{(\gamma-1)/\gamma} - 1\right] + 1}} \tag{A8}$$

For a given free-stream Mach number and adiabatic efficiency, the ratio of C_Q/C_T varies only with engine pressure ratio as illustrated in figure 2.

REFERENCES

1. Spence, D. A.: The Lift Coefficient of a Thin, Jet-Flapped Wing. Proc. Roy. Soc. (London), Ser. A, vol. 238, no. 1212, Dec. 4, 1956, pp. 46-68.

2. Spence, D. A.: The Lift on a Thin Aerofoil with Jet-Augmented Flap. Aeron. Quart., vol. 9, Aug. 1958, pp. 289-299.

3. Albers, James A.; and Potter, Merle C.: Potential Flow Solution for a STOL Wing Propulsion System. NASA TN D-6394, 1971.

4. Giesing, Joseph P.: Extension of the Douglas Neumann Program to Problems of Lifting Infinite Cascades. Rep. LB-31653, Douglas Aircraft Co., July 2, 1964. (Available from DDC as AD-605207.)

5. Hess, J. L.; and Smith, A. M. O.: Calculation of Potential Flow About Arbitrary Bodies. Progress in Aeronautical Sciences. Vol. 8, D. Küchemann, ed., Pergamon Press, 1967, pp. 1-138.

6. Albers, James A.: Two-Dimensional Potential Flow and Boundary Layer Analysis on the Airfoil of a STOL Wing Propulsion System. Ph. D. Thesis, Michigan State Univ., 1971.

7. Smith, Charles C., Jr.: Effect of Engine Position and High-Lift Devices on Aerodynamic Characteristics of an External-Flow Jet-Flap STOL Model. NASA TN D-6222, 1971.

8. Williams, J.; Butler, F. J.; and Wood, M. N.: The Aerodynamics of Jet Flaps. Rep. R&M 3304, Aeronautical Research Council, Gt. Britain, 1963.

9. Yuska, Joseph A.; Diedrich, James H.; and Clough, Nestor: Lewis 9-by-15-Foot V/STOL Wind Tunnel. NASA TM X-2305, 1971.

10. Sanders, Newell D.; Diedrich, James H.; Hassell, James L., Jr.; Hickey, David H.; Luidens, Roger W.; and Stewart, Warner L.: V/STOL Propulsion. Aircraft Propulsion. NASA SP-259, 1971, pp. 135-168.

11. Foster, D. N.: The Flow Around Wing Sections with High-Lift Devices. Paper 71-96, AIAA, Jan. 1971.

12. Shapiro, Ascher H.: The Dynamics and Thermodynamics of Compressible Fluid Flow. Vol. I. Ronald Press, 1953.

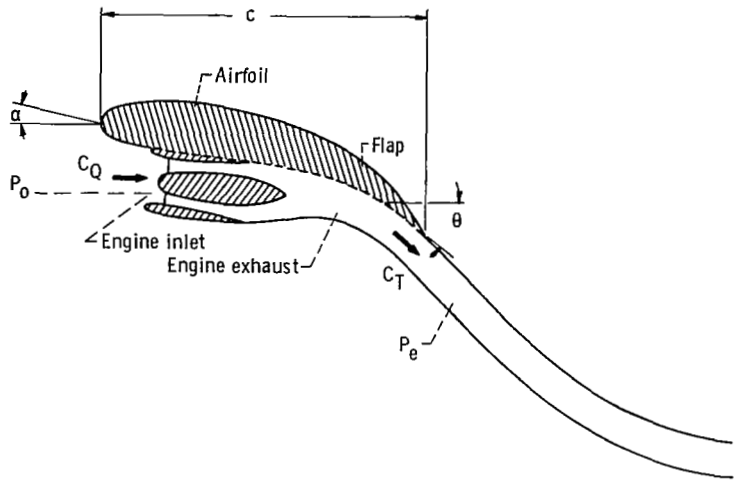

Figure 1. - Two-dimensional representation of wing propulsion system.

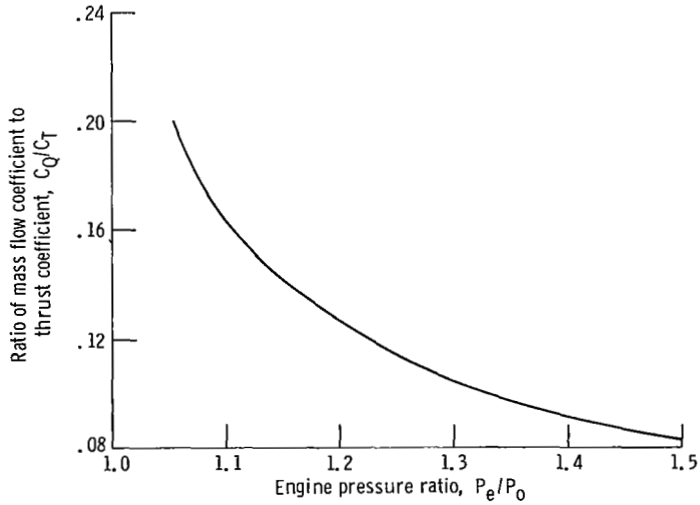

Figure 2. - Relation of propulsion system parameters to engine pressure ratio. Free-stream Mach number, $M_\infty = 0.12$; adiabatic efficiency, $\eta = 0.85$.

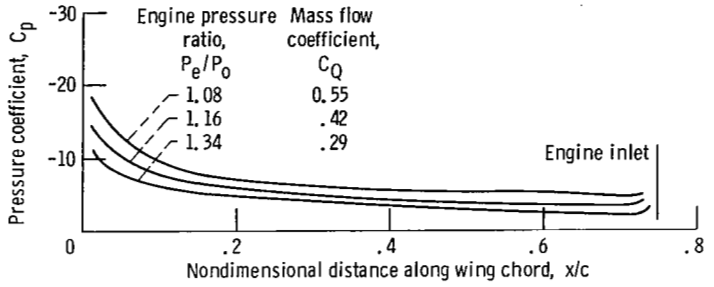

(a) Upper surface pressure distribution.

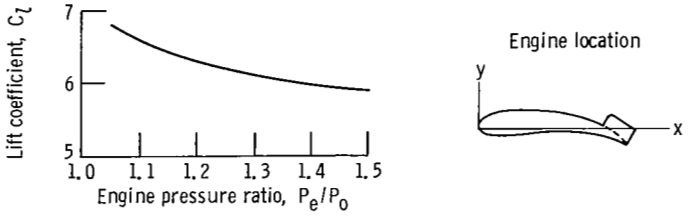

(b) Lift coefficient.

Figure 3. - Effect of engine pressure ratio on upper surface pressure distribution and lift coefficient for constant thrust coefficient and engines on top of flap; thrust coefficient, 3.

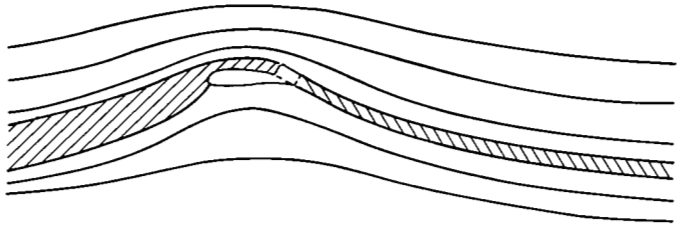

(a) Engine pressure ratio, 1.34; mass flow coefficient, 0.29.

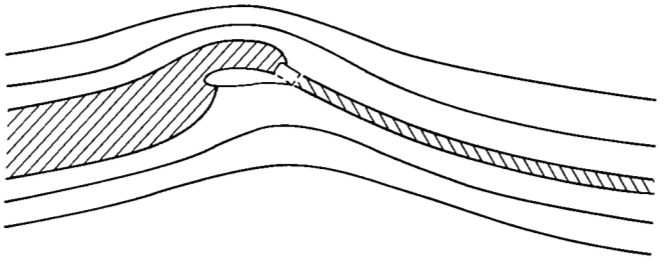

(b) Engine pressure ratio, 1.05; mass flow coefficient, 0.63.

Figure 4. - Comparison of flow fields at various engine pressure ratios for constant thrust coefficient and engines on top of flap. Thrust coefficient, 3.

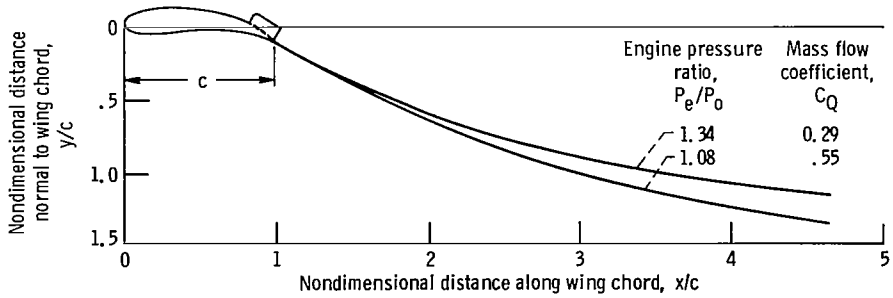

Figure 5. - Effect of engine pressure ratio on jet penetration for constant thrust coefficient of 3.

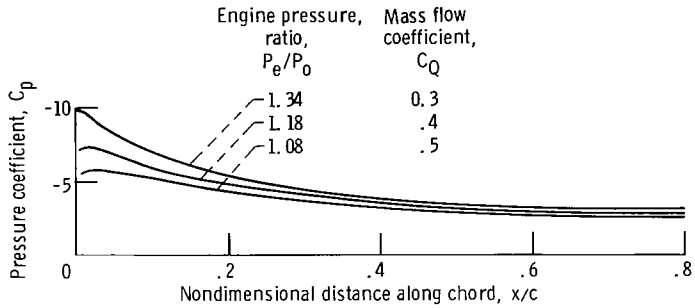

(a) Upper surface pressure distribution.

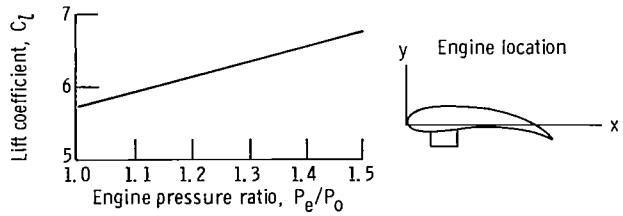

(b) Lift coefficient.

Figure 6. - Effect of engine pressure ratio on upper surface pressure distribution and lift coefficient for constant thrust coefficient and engines under wing. Thrust coefficient, 3.

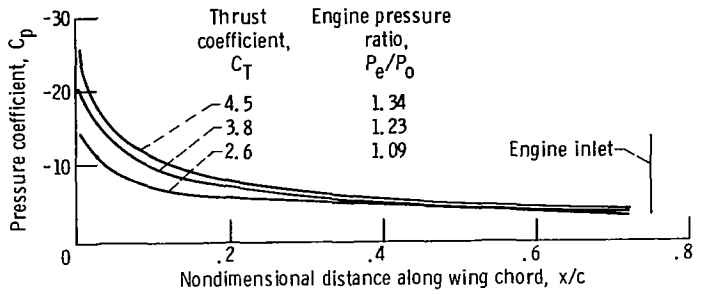

(a) Upper surface pressure distribution.

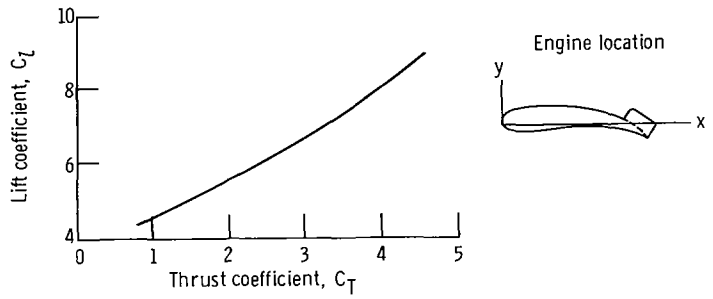

(b) Lift coefficient.

Figure 7. - Effect of thrust coefficient on upper surface pressure distribution and lift coefficient for constant mass flow coefficient and engines on top of flap. Mass flow coefficient, 0.45.

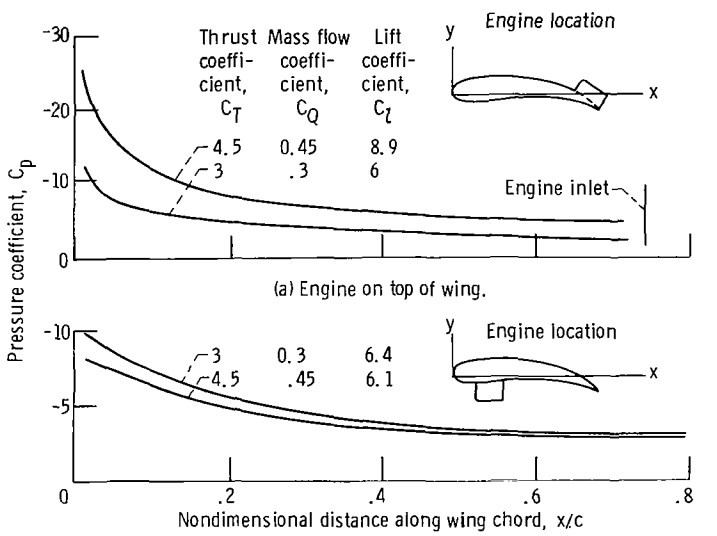

(a) Engine on top of wing.

(b) Engine on bottom of wing.

Figure 8. - Effect of mass flow coefficient and thrust coefficient on upper surface pressure distribution and lift coefficient for constant engine pressure ratio of 1.34.

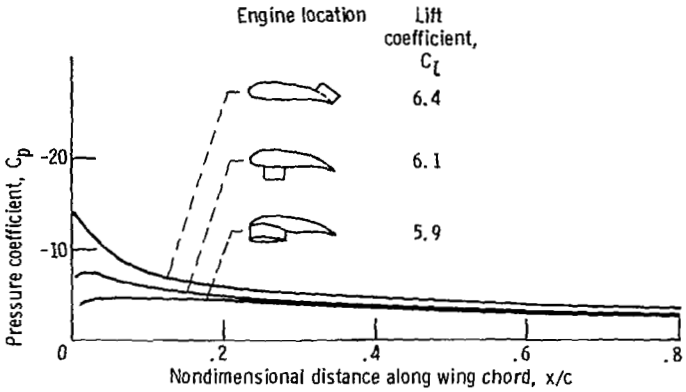

Figure 9. - Comparison of pressure distributions at various engine locations at constant engine pressure ratio of 1.18. Thrust coefficient, 3; mass flow coefficient, 0.4.

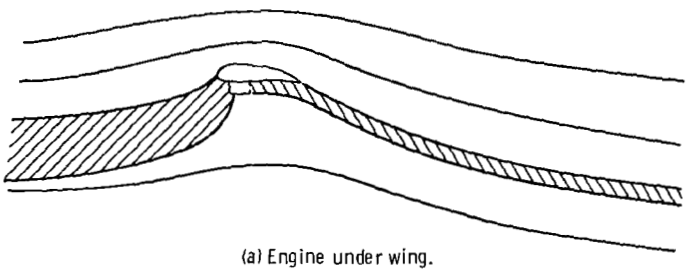

(a) Engine under wing.

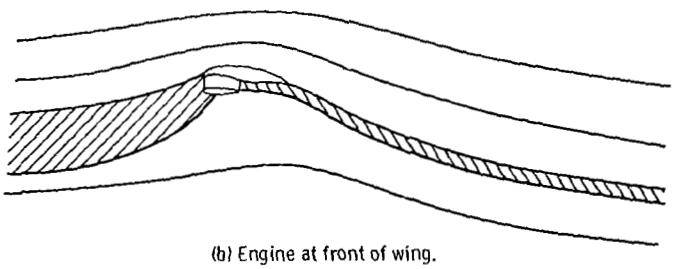

(b) Engine at front of wing.

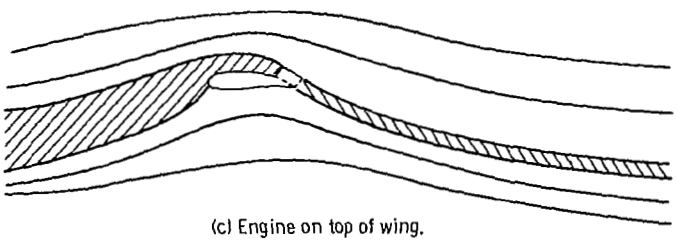

(c) Engine on top of wing.

Figure 10. - Comparison of flow field at various engine locations at constant engine pressure ratio of 1.18. Thrust coefficient, 3; mass flow coefficient, 0.4.

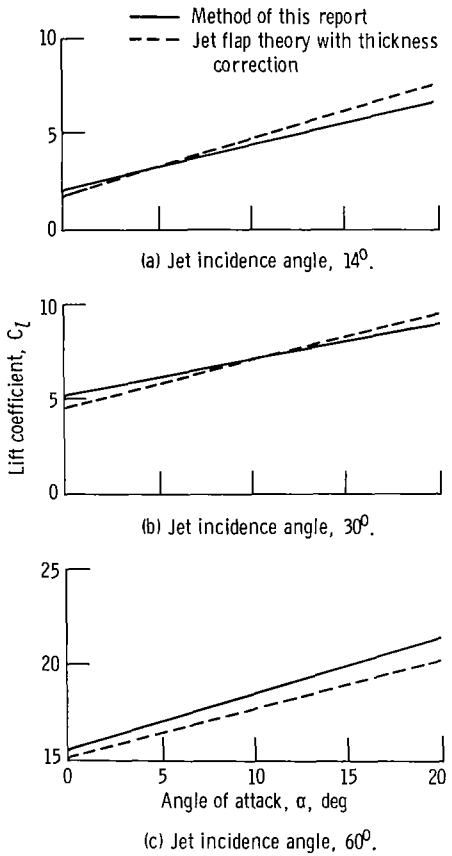

(a) Jet incidence angle, 14°.

(b) Jet incidence angle, 30°.

(c) Jet incidence angle, 60°.

Figure 11. - Comparison of theoretical two-dimensional lift coefficients. Thrust coefficient, 3; no engine; mass flow coefficient, 0.

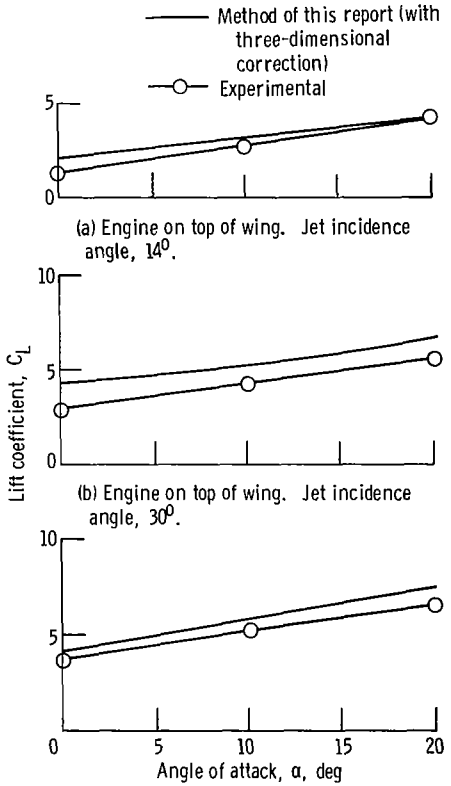

(a) Engine on top of wing. Jet incidence angle, 14°.

(b) Engine on top of wing. Jet incidence angle, 30°.

(c) Engine on bottom of wing. Jet incidence angle, 30°.

Figure 12. - Comparison of calculated and experimental three-dimensional lift coefficients. Thrust coefficient, 3; mass flow coefficient, 0.44; engine pressure ratio, 1.18.

"The aeronautical and space activities of the United States shall be conducted so as to contribute . . . to the expansion of human knowledge of phenomena in the atmosphere and space. The Administration shall provide for the widest practicable and appropriate dissemination of information concerning its activities and the results thereof."

— NATIONAL AERONAUTICS AND SPACE ACT OF 1958

NASA SCIENTIFIC AND TECHNICAL PUBLICATIONS

TECHNICAL REPORTS: Scientific and technical information considered important, complete, and a lasting contribution to existing knowledge.

TECHNICAL NOTES: Information less broad in scope but nevertheless of importance as a contribution to existing knowledge.

TECHNICAL MEMORANDUMS: Information receiving limited distribution because of preliminary data, security classification, or other reasons.

CONTRACTOR REPORTS: Scientific and technical information generated under a NASA contract or grant and considered an important contribution to existing knowledge.

TECHNICAL TRANSLATIONS: Information published in a foreign language considered to merit NASA distribution in English.

SPECIAL PUBLICATIONS: Information derived from or of value to NASA activities. Publications include conference proceedings, monographs, data compilations, handbooks, sourcebooks, and special bibliographies.

TECHNOLOGY UTILIZATION PUBLICATIONS: Information on technology used by NASA that may be of particular interest in commercial and other non-aerospace applications. Publications include Tech Briefs, Technology Utilization Reports and Technology Surveys.

Details on the availability of these publications may be obtained from:

SCIENTIFIC AND TECHNICAL INFORMATION OFFICE

NATIONAL AERONAUTICS AND SPACE ADMINISTRATION

Washington, D.C. 20546